

Isoscalar mesons upon unbreaking of chiral symmetry

M. Denissenya,^{*} L.Ya. Glozman,[†] and C.B. Lang[‡]
Institute of Physics, University of Graz, A-8010 Graz, Austria

In a dynamical lattice simulation with the overlap Dirac operator and $N_f = 2$ mass degenerate quarks we study all possible $J = 0$ and $J = 1$ correlators upon exclusion of the low lying “quasi-zero” modes from the valence quark propagators. After subtraction of a small amount of such Dirac eigenmodes all disconnected contributions vanish and all possible point-to-point $J = 0$ correlators with different quantum numbers become identical, signaling a restoration of the $SU(2)_L \times SU(2)_R \times U(1)_A$. The original ground state of the π meson does not survive this truncation, however. In contrast, in the $I = 0$ and $I = 1$ channels for the $J = 1$ correlators the ground states have a very clean exponential decay. All possible chiral multiplets for the $J = 1$ mesons become degenerate, indicating a restoration of an $SU(4)$ symmetry of the dynamical QCD-like string.

PACS numbers: 12.38.Gc, 11.25.-w, 11.30.Rd

I. INTRODUCTION

In Ref. [1] we have studied the behavior of masses of the isovector $J = 1$ mesons ρ, ρ', a_1, b_1 upon subtraction of the lowest-lying eigenmodes of the manifestly chirally-invariant overlap Dirac operator [2] from the valence quark propagators (for a previous lattice study with a chirally-improved Dirac operator see Refs. [3, 4]). A non-vanishing density of the quasi-zero modes of the Dirac operator (in the infinite volume limit) represents, through the Banks-Casher relation [5], the quark condensate of the vacuum. Consequently, a removal of a sufficient amount of the lowest-lying Dirac eigenmodes should eventually lead to the artificial restoration (“unbreaking”) of chiral symmetry.

Of course, correlators obtained after such a truncation do not correspond to a local quantum field theory [6] and we call that case QCD_r in order to distinguish it from the full, untruncated QCD. Despite that fact the correlators shown intriguing behavior. Firstly, they have a very clean exponential decay for all isovector $J = 1$ mesons, suggesting that these states survive the unbreaking procedure. Secondly, they have interesting symmetry patterns: All ρ, ρ', a_1, b_1 states become degenerate. Certainly this degeneracy is not accidental and tells us something important about the underlying dynamics. From this degeneracy we could infer a simultaneous restoration of both $SU(2)_L \times SU(2)_R$ and $U(1)_A$ symmetries. However, a degeneracy of all isovector states implies a larger symmetry that includes $SU(2)_L \times SU(2)_R$ and $U(1)_A$ as subgroups. This larger symmetry would require a degeneracy of all possible chiral multiplets that contain both isovector and isoscalar $J = 1$ mesons. One of the principal purposes of the present study is to investigate the isoscalar $J = 1$ states from all possible chiral multiplets and clarify whether they become degenerate upon un-

breaking of the chiral symmetry.

This larger symmetry has been identified in Ref. [8] as an $SU(4) \supset SU(2)_L \times SU(2)_R \times U(1)_A$, that mixes components of the fundamental four-component vector (u_L, u_R, d_L, d_R) . This symmetry, which is a symmetry of the confining interaction in QCD_r , is not a symmetry of the original QCD Lagrangian and should be considered as an emergent symmetry that appears from the QCD dynamics upon subtraction of the quasi-zero modes of the Dirac operator. From the degeneracy of all possible $J = 1$ chiral multiplets and from this symmetry it was possible to conclude that there is no color-magnetic field in the system suggesting that we observe quantum levels of a dynamical QCD_r string.

Our second aim in the present paper is to study the fate of the ground states of the π, σ, a_0, η mesons upon unbreaking of the chiral symmetry. One naturally expects a disappearance of the pion as a Goldstone boson from the spectrum. However, a priori it is not clear what behavior to expect for the other $J = 0$ mesons. We find that the disconnected contributions vanish and that the point-to-point correlation functions in all $J = 0$ channels become indistinguishable after removal of the lowest-lying modes. This confirms a restoration of the $SU(2)_L \times SU(2)_R$ and $U(1)_A$ symmetries. The eigenvalues of the correlation matrices that correspond to the ground states of π, σ, a_0, η mesons loose, however, the exponential decay property implying that the unbreaking removes the physical ground states of π, σ, a_0, η mesons from the spectrum.

II. LATTICE TECHNIQUES

A. Quark propagators

As was discussed in the Introduction we use in our study the overlap Dirac operator. The gauge ensemble consists of 100 gauge configurations generated with $N_f = 2$ mass degenerate dynamical overlap fermions on a $16^3 \times 32$ lattice with a lattice spacing $a \sim 0.12$ fm [9, 10]. The

^{*}Electronic address: mikhail.denissenya@uni-graz.at

[†]Electronic address: leonid.glozman@uni-graz.at

[‡]Electronic address: christian.lang@uni-graz.at

gauge configurations were generated by constraining the simulation always to the same topological sector $Q_T = 0$. The effect of this was discussed in Ref. [11]. While it is known that there is a slight dependence $O(1/V)$ of the bound state masses on the topological sector [12] it is expected to be very small [13] compared to our statistical error and should become irrelevant in the infinite volume limit.¹

The pion mass in this ensemble is $M_\pi = 289(2)$ MeV [14]. The overlap quark propagators and gauge configurations were generously provided by the JLQCD collaboration [9, 10, 14]. The quark propagators were computed by the combining of the exact 100 low modes (eigenvectors of the Dirac operator) with the stochastic estimates for the higher modes, (see Appendix A for details).

To unbreak the chiral symmetry we exclude the lowest-lying modes from the valence quark propagators. We introduce the reduced valence quark propagators using the spectral representation where an increasing number k of the near-zero modes is excluded from the full propagator:

$$S_k(x, y) = \sum_{n=k+1}^{100} \frac{1}{\lambda_n} u_n(x) u_n^\dagger(y) + S_{Stoch} \quad (1)$$

Full (not reduced) quark propagators correspond to $k = 0$ and all reduced to $k > 0$.

B. Meson observables

Meson spectroscopy is done by means of the standard variational approach [16]. In each channel we use a set of interpolators with all possible chiral structures [17], see Table I. Each of these operators is constructed from quark propagators with smeared sources. The exponential type of smearing with a set of different smearing parameters is used at the source/sink and summarized in Appendix A (for the computational techniques see [10, 15]). This way we have several interpolators in each quantum channel and can use the variational method.

After construction of the cross-correlation matrices

$$C_{ij}(t) = \langle 0 | \mathcal{O}_i(t) \mathcal{O}_j^\dagger(0) | 0 \rangle \quad (2)$$

with the size of the matrices C_{ij} ranging from 5×5 to 10×10 we solve the generalized eigenvalue problem

$$C(t) \vec{v}_n(t) = \tilde{\lambda}^{(n)}(t) C(t_0) \vec{v}_n(t_0). \quad (3)$$

Resulting masses of the states are obtained by identifying the exponential behavior of the eigenvalues $\tilde{\lambda}^{(n)}(t, t_0) = e^{-E_n(t-t_0)} (1 + \mathcal{O}(e^{-\Delta E_n(t-t_0)}))$ with $t_0 = 1$. Such

¹In our previous study without fixing topological charge [4] the observed symmetries were noted as well, although with less precision.

states are extracted for each truncation level k in a given quantum channel.

I, J^{PC}	\mathcal{O}	R
$\pi(1, 0^{-+})$	$\bar{q}\gamma_5 \frac{\vec{\tau}}{2} q$	$(1/2, 1/2)_a$
$\eta(0, 0^{-+})$	$\bar{q}\gamma_5 q$	$(1/2, 1/2)_b$
$a_0(1, 0^{++})$	$\bar{q} \frac{\vec{\tau}}{2} q$	$(1/2, 1/2)_b$
$\sigma(0, 0^{++})$	$\bar{q} q$	$(1/2, 1/2)_a$
$\rho(1, 1^{--})$	$\bar{q}\gamma_i \frac{\vec{\tau}}{2} q$ $\bar{q}\gamma_i \gamma_t \frac{\vec{\tau}}{2} q$	$(1, 0) + (0, 1)$ $(1/2, 1/2)_b$
$\omega(0, 1^{--})$	$\bar{q}\gamma_i q$ $\bar{q}\gamma_i \gamma_t q$	$(0, 0)$ $(1/2, 1/2)_a$
$a_1(1, 1^{++})$	$\bar{q}\gamma_i \gamma_5 \frac{\vec{\tau}}{2} q$	$(1, 0) + (0, 1)$
$f_1(0, 1^{++})$	$\bar{q}\gamma_i \gamma_5 q$	$(0, 0)$
$b_1(1, 1^{+-})$	$\bar{q}\gamma_i \gamma_j \frac{\vec{\tau}}{2} q$	$(1/2, 1/2)_a$
$h_1(0, 1^{+-})$	$\bar{q}\gamma_i \gamma_j q$	$(1/2, 1/2)_b$

TABLE I: $J = 0$ and $J = 1$ meson interpolating fields with the corresponding chiral representation R .

III. RESULTS

A. $J = 0$ mesons

The symmetry connections between the $J = 0$ interpolators [18] are shown in Fig. 1. If both the $SU(2)_L \times SU(2)_R$ and $U(1)_A$ symmetries get restored we should observe, on the one hand, a coincidence of the point-to-point correlators obtained with all these four operators. On the other hand, if there are physical states with the corresponding quantum numbers, i.e., π, σ, a_0, η , they must be degenerate. One should stress that a coincidence of the point-to-point correlators does not imply yet existence of the degenerate physical states. Only if the eigenvalues of the correlation matrices show an exponential decay at large time one can speak about the states.

$$\begin{array}{ccc}
 (1/2, 1/2)_a: & \pi(\bar{q}\gamma_5 \frac{\vec{\tau}}{2} q) & \xleftrightarrow{SU(2)_L \times SU(2)_R} \sigma(\bar{q}q) \\
 & U(1)_A \updownarrow & \updownarrow U(1)_A \\
 (1/2, 1/2)_b: & a_0(\bar{q} \frac{\vec{\tau}}{2} q) & \xleftrightarrow{SU(2)_L \times SU(2)_R} \eta(\bar{q}\gamma_5 q)
 \end{array}$$

FIG. 1: Symmetry relations among $J = 0$ interpolators.

In general there are two distinct contributions to the correlation functions depending on the isospin I [19, 20]. The isovector correlation functions contain only connected (C) contributions. Both the connected and disconnected (D) diagrams contribute to the isoscalar mesons, see Fig. 2. The difference between the isoscalar

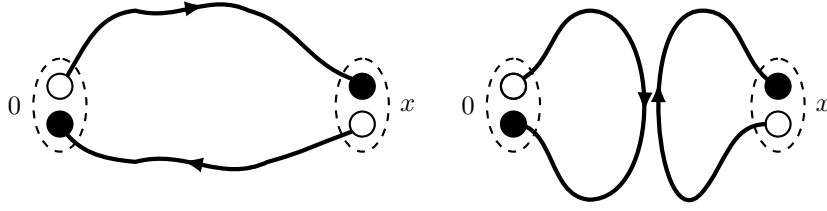


FIG. 2: Connected (left) and disconnected (right) contributions to meson correlators.

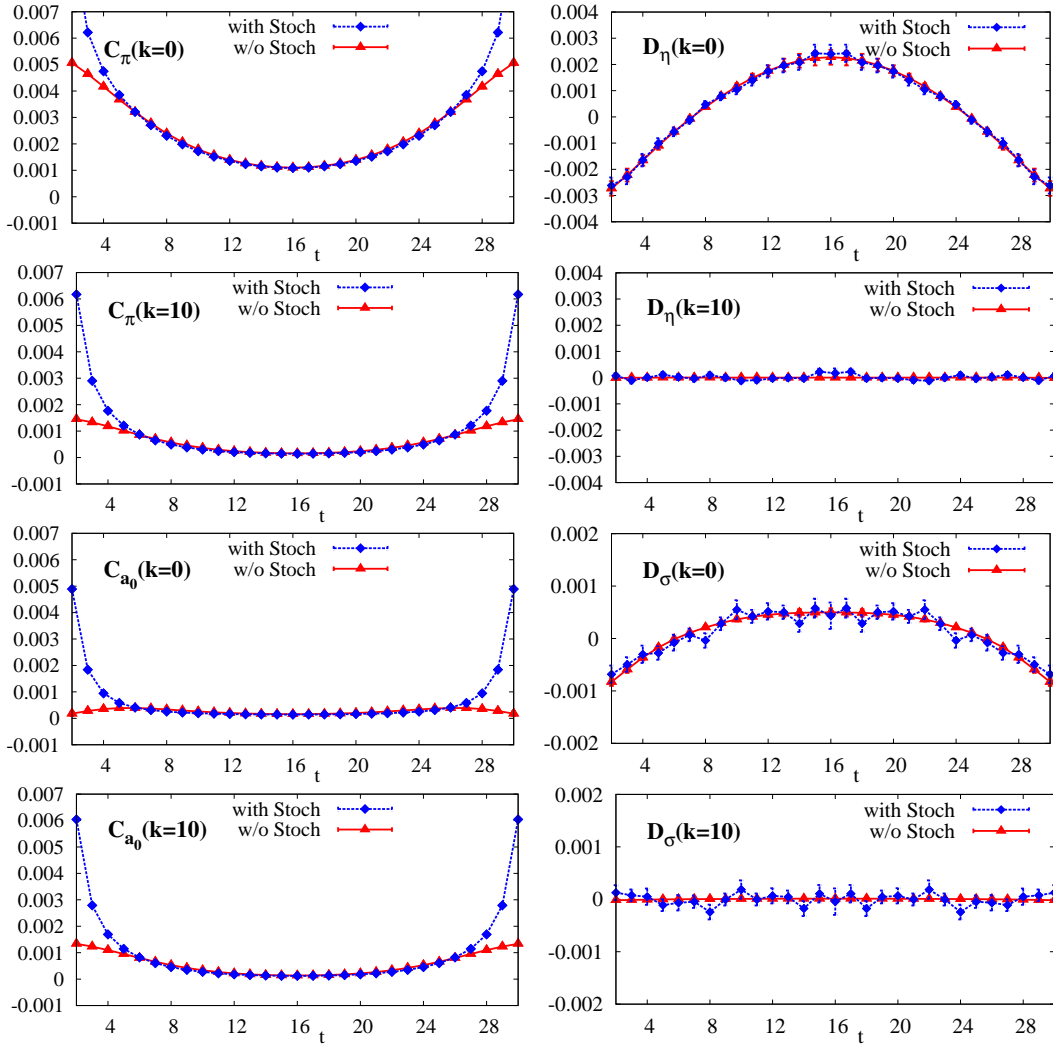


FIG. 3: Connected (left) and disconnected (right) contributions to the η and σ meson correlators with included or excluded stochastically estimated part of the quark propagator, $k = 0, 10$.

and isovector channels with the same parity, i.e., between η and π , as well as between σ and a_0 is described by the contribution $D(t)$ coming from the disconnected diagrams:

$$F_{\eta(\sigma)} = C_{\pi(a_0)} + D_{\eta(\sigma)}, \quad (4)$$

where F is the full correlator.

A subtraction of the quasi-zero modes of the Dirac operator should naturally lead to the restoration of the chiral $SU(2)_L \times SU(2)_R$ symmetry since these modes are connected to the quark condensate of the vacuum. Consequently, upon unbreaking of the chiral symmetry one expects a coincidence of the π and σ as well as of the a_0 and η correlators. However, one does not know a priori what will happen with the $U(1)_A$ symmetry. If the chi-

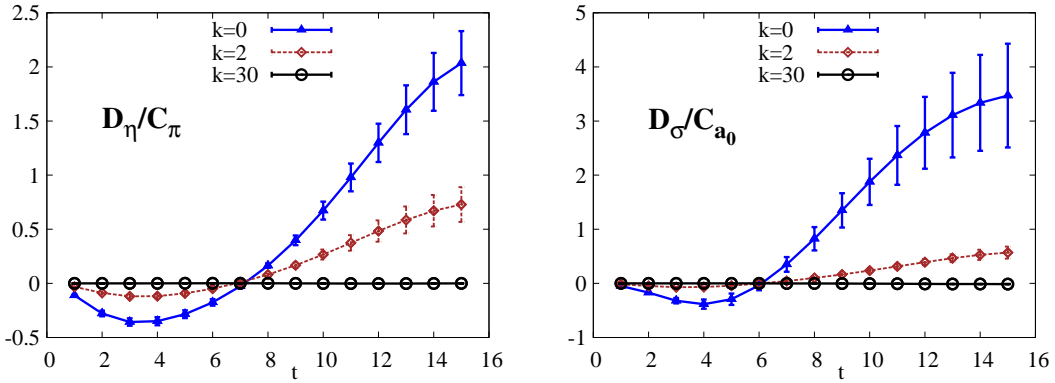


FIG. 4: Ratios of disconnected (without stochastic contribution) and connected $J = 0$ correlators, $k = 0, 2, 30$.

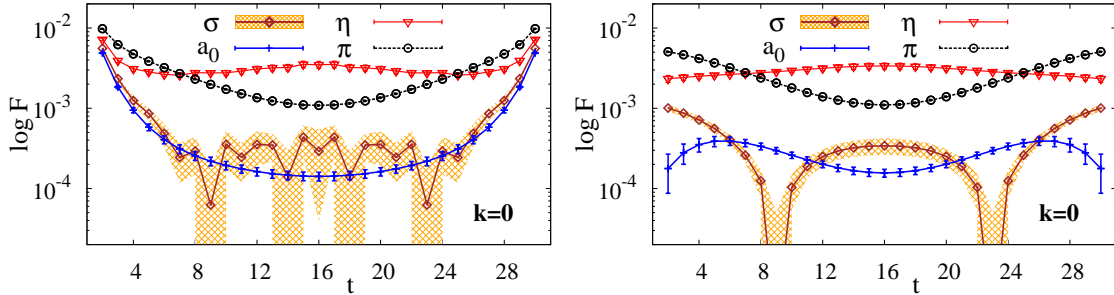


FIG. 5: π , σ , a_0 , η correlators with stochastic contributions (left), without stochastic contributions (right) without exclusion of the near-zero modes, $k = 0$.

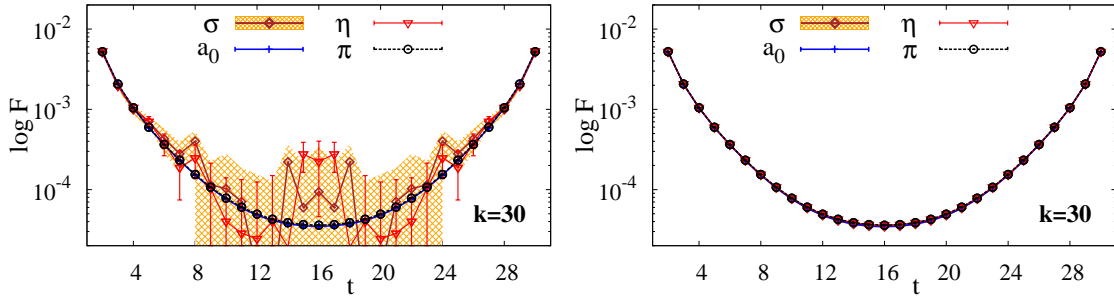


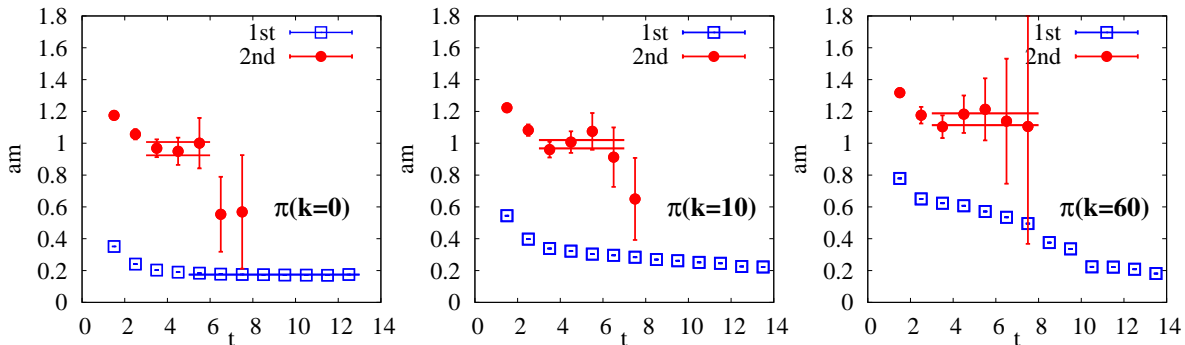
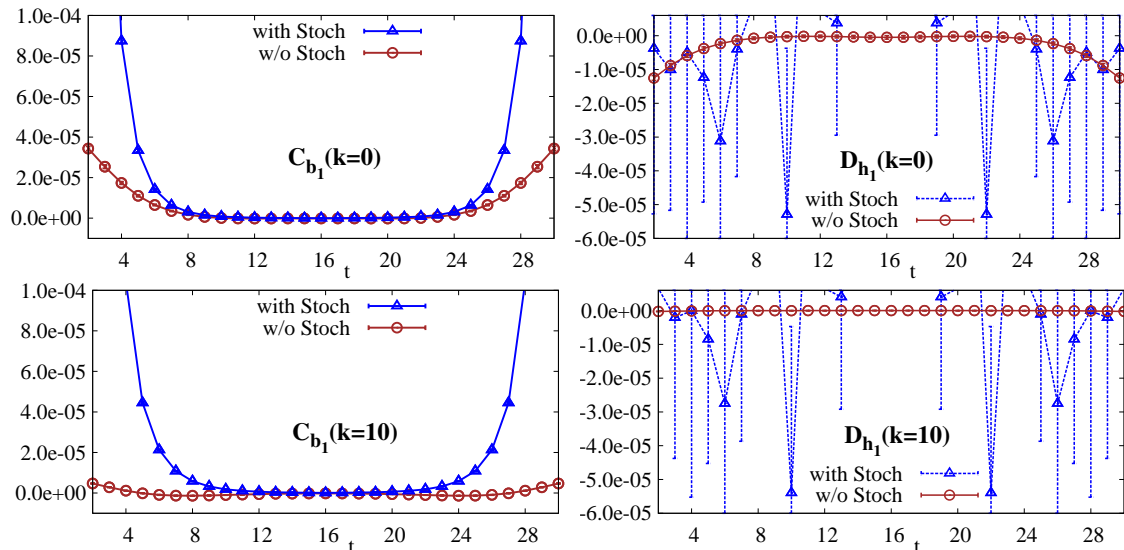
FIG. 6: π , σ , a_0 , η correlators with stochastic contributions (left), without stochastic contributions to disconnected pieces (right) upon exclusion of the near-zero modes, $k = 30$.

ral symmetry is restored but the $U(1)_A$ symmetry is still broken the π and η correlators should be different, i.e., the η disconnected contributions should not vanish. If, on the contrary, the same low-lying modes are responsible for both $SU(2)_L \times SU(2)_R$ and $U(1)_A$ breaking, one expects that the η disconnected contributions should vanish upon elimination of the lowest-lying Dirac modes.

Hence, it is instructive to study the behavior of the connected and disconnected correlators upon exclusion of the near-to-zero modes separately from each other. In Fig. 3 we show the connected (π) and disconnected (η) contributions for untruncated correlators ($k = 0$) and after subtraction of 10 lowest eigenmodes of the Dirac op-

erator ($k = 10$). It is clearly seen that in the untruncated case both the connected and disconnected contributions are equally important, which provides an essential difference of the π and η masses. Actually, for the η propagator they almost cancel, prohibiting a determination of the mass. This is due to the fixing of the global topological charge which leads to a vanishing topological susceptibility χ_T (In Ref. [21] it is discussed how to estimate χ_T in this case from the disconnected part of the η correlator).

In the figures we exhibit both, the propagators with and without the stochastic contributions to the quark propagators (see Eq. (1)). We see, that the stochastic part is very small beyond $t > 5$ and negligible for the

FIG. 7: π effective masses at $k = 0, 10, 60$.FIG. 8: Connected (left) and disconnected (right) contributions to h_1 meson correlator with included or excluded stochastically estimated part of the quark propagator, $k = 0, 10$.

disconnected parts. The dependence of the disconnected parts with truncation is remarkable. Upon elimination of 10 lowest Dirac eigenmodes the disconnected contribution practically vanishes. This signals a simultaneous restoration of both symmetries.

The same observation holds for the connected and disconnected contributions in the a_0 and σ channels. The ratios of the corresponding contributions are shown in Fig. 4. We conclude that the same lowest-lying eigenmodes of the Dirac operator are responsible for both $SU(2)_L \times SU(2)_R$ and $U(1)_A$ breakings which is consistent with the instanton-induced mechanism of both breakings [23–25].

The total (F) point-to-point correlators in all π, σ, a_0, η channels are shown in Fig. 5-6. For the untruncated case we see again by comparing the plots in Fig. 5 left to right, that the stochastic contribution is relevant for small distances and responsible for the increased noise in the σ correlation. For the truncated case (Fig. 6) the results agree whether one includes the stochastic contribution or not. An exception is again the σ where the noise due to

the stochastic term shadows the large distance behavior. The unusual shape of the η correlator is due to the fixing of the global topological as discussed in Ref. [10]. Without truncation of the lowest-lying Dirac modes the correlators are all very different due to breakings of both $SU(2)_L \times SU(2)_R$ and $U(1)_A$ symmetries. After truncation of a small amount of the quasi-zero modes they become all almost identical. This tells once again that both symmetries are restored.

The next natural question is to ask whether the states still exist as physical states in this chirally restored regime. To answer this question we concentrate on the pion channel for the following reason: The original π states can be easily identified in the untruncated case. Extraction of good effective mass plateaus in other quantum channels requires much better statistics.

On exclusion of the near-zero modes the ground state effective mass plateau of the pion deteriorates and disappears, see Fig. 7. The correlation function decays with time not exponentially and thus the eigenstate is not a physical state. Hence unbreaking of the chiral symmetry

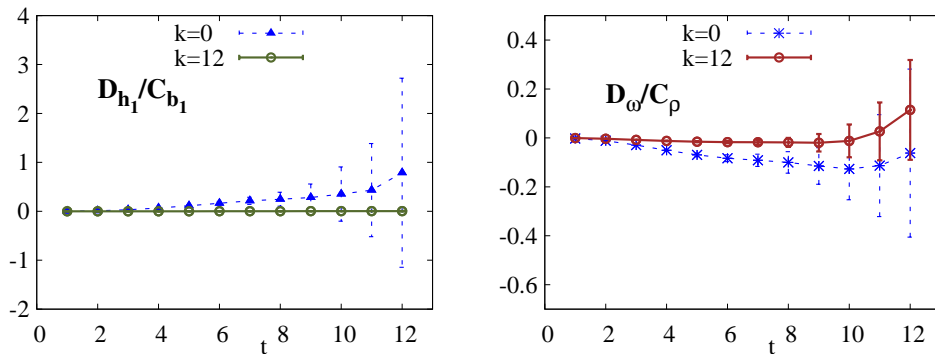


FIG. 9: Ratios of the disconnected and connected $J = 1$ correlators, $k = 0, 12$.

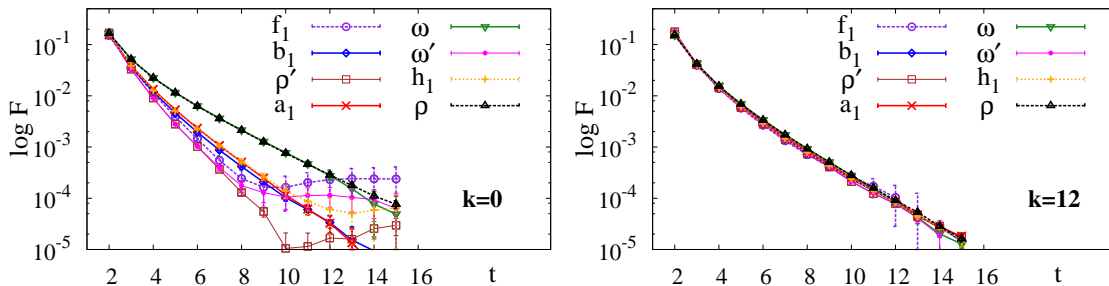


FIG. 10: $J = 1$ correlators without truncation (left) and upon exclusion of the near-zero modes, $k = 12$ (right).

removes the pion from the physical spectrum. This is consistent with the Goldstone boson nature of the pion. The quasi-zero modes play an important role in the pion and are crucial for its existence. The π' state might however survive the unbreaking, though to firmly conclude it one needs better statistics.

A sufficient condition for a symmetry restoration is a coincidence of the correlators obtained with the operators that are connected by the symmetry transformation. From the results presented above it then follows that the $SU(2)_L \times SU(2)_R$ and $U(1)_A$ symmetry in the $J = 0$ sector is restored upon unbreaking. Existence or nonexistence of the bound states in the symmetry restored regime is the other question. If at a given energy at least in one of the channels there is no bound state, then the symmetry requires that there must not be bound states at the same energy in all other $J = 0$ channels. The pion does not survive the unbreaking. Consequently there cannot be respective σ, a_0, η bound states after unbreaking. The excited π' state might survive, however. If it does, there must be then degenerate $\pi', \sigma', a'_0, \eta'$ states in the spectrum.

B. $J = 1$ mesons

Like the isoscalar $J = 0$ mesons, the isoscalar $J = 1$ mesons also contain both connected and disconnected contributions. In contrast to the $J = 0$ channels, the dis-

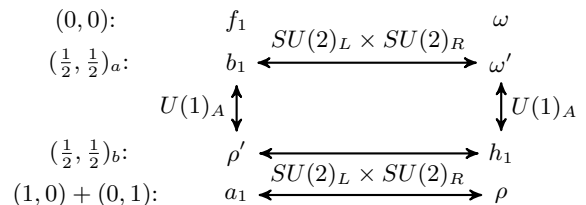


FIG. 11: Symmetry relations among $J = 1$ mesons [18, 22].

connected contributions in the $J = 1$ case are small compared to the connected ones. Indeed, the ground states of ρ and ω mesons are approximately degenerate in Nature. Microscopically their splitting is due to contributions of the disconnected graphs. Hence the latter contributions have to be small compared to the connected ones. The most likely interpretation is that these disconnected diagrams are supported in the infrared by the instantons, i.e., by the 't Hooft vertex. This vertex is limited, however, to the $J = 0$ channel. Consequently, while for the $J = 0$ mesons a removal of the lowest Dirac eigenmodes from the valence quarks diminishes the otherwise large disconnected contributions, for the spin $J = 1$ mesons we should not expect any significant changes in the disconnected correlators.

The disconnected contributions for $J = 1$ are small, very noisy and suffer from large fluctuations, see Fig. 8. From the results in the $J = 0$ sector we have seen

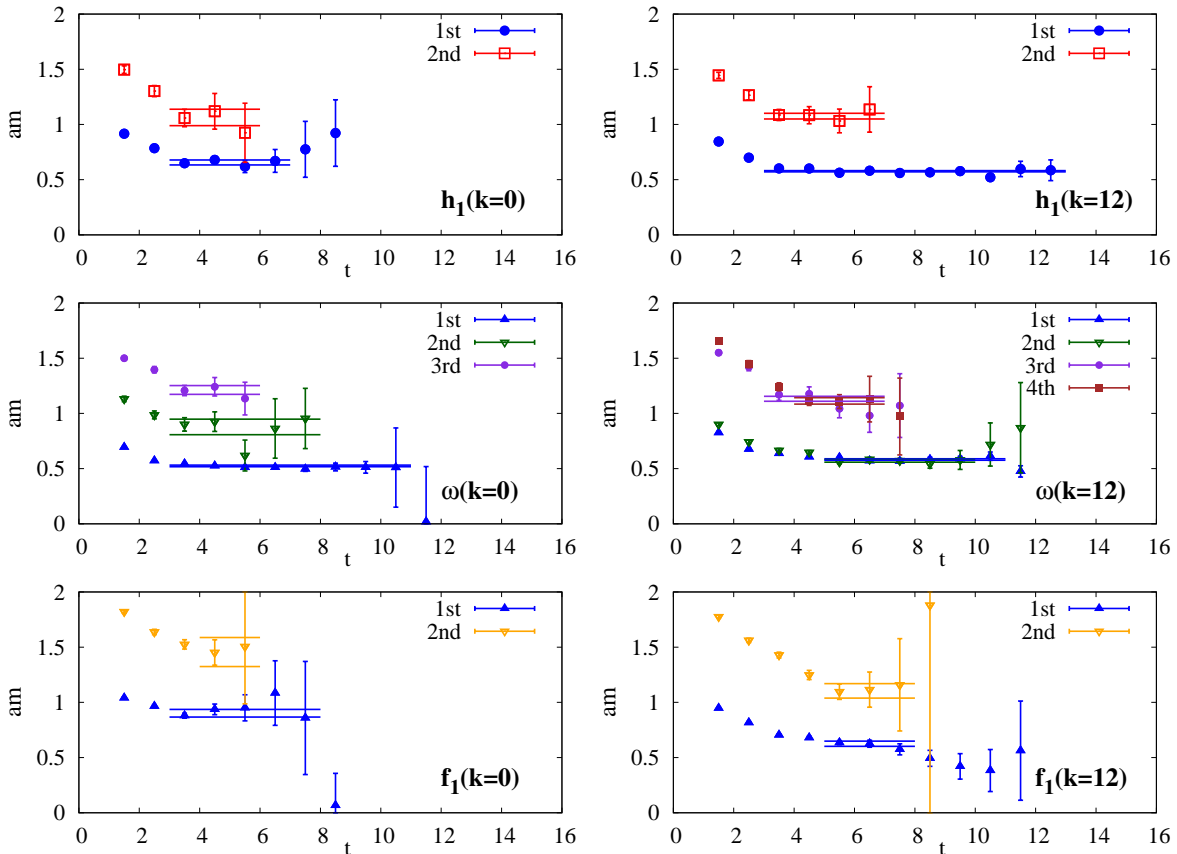


FIG. 12: Effective masses for h_1, ω, f_1 isoscalars.

that the contributions to the disconnected terms from the stochastic part are negligibly small. Consequently, we have decided to omit the small but very noisy stochastically estimated contribution of the high-lying modes to the disconnected correlators and discuss in this case only the exactly calculated contribution coming from the lowest 100 modes.

In Fig. 9 we show the ratio of the disconnected to the connected contribution in the h_1 correlator. The connected h_1 and b_1 contributions coincide. We see that the disconnected contribution is very small even for the “untruncated” case $k = 0$ and vanishes practically completely upon removal of the lowest 12 Dirac eigenmodes. A similar behavior is found in other $J = 1$ isoscalar channels.

The point-to-point correlators obtained with the $J = 1$ operators from the Table 1 are shown in Fig. 10. The symmetry connections between these operators are illustrated in Fig. 11. A coincidence of the correlators in the $\rho - a_1, b_1 - \omega'$ and $h_1 - \rho'$ pairs evidences a restoration of $SU(2)_L \times SU(2)_R$. The equality of the h_1, ρ', b_1, ω' correlation functions demonstrates the $SU(2)_L \times SU(2)_R \times U(1)_A$ symmetry. A coincidence of all eight correlators tells about some higher symmetry; we will return to this question below.

Now we turn to the discussion of the bound states in

all these channels. The bound states of the isovector mesons ρ, ρ', a_1, b_1 have been shown in our previous paper [1]. Fig. 12 demonstrates effective mass plateaus for all isoscalar $J = 1$ mesons upon truncation of the lowest-lying Dirac eigenmodes. We see a reliable mass plateau for the ground state h_1 , which significantly improves upon truncation of the lowest eigenmodes. Upon unbreaking of chiral symmetry the ground ω -state and its first excitation ω' get degenerate. It is similar to what happens to ρ and ρ' states [1].

All final results for masses, obtained from the one-exponential fits to the eigenvalues of the cross-correlation matrices are shown in Fig. 13. The fit ranges, the extracted masses with their errors are given in the Appendix B in Table III.

We see a degeneracy in all possible chiral multiplets of the $J = 1$ mesons (see Fig. 11): $\rho - a_1, b_1 - \omega'$ and $h_1 - \rho'$. This evidences a restoration of $SU(2)_L \times SU(2)_R$. Simultaneously the $U(1)_A$ symmetry gets also restored, because all four mesons h_1, ρ', b_1, ω' are degenerate. A degeneracy of all eight $J = 1$ mesons indicates a restoration of an even higher symmetry $SU(4) \supset SU(2)_L \times SU(2)_R \times U(1)_A$ [8]. The transformations of the latter mix the components of the fundamental four-component vector (u_L, u_R, d_L, d_R) . The high degeneracy of the energy levels and the $SU(4)$ symmetry imply absence of

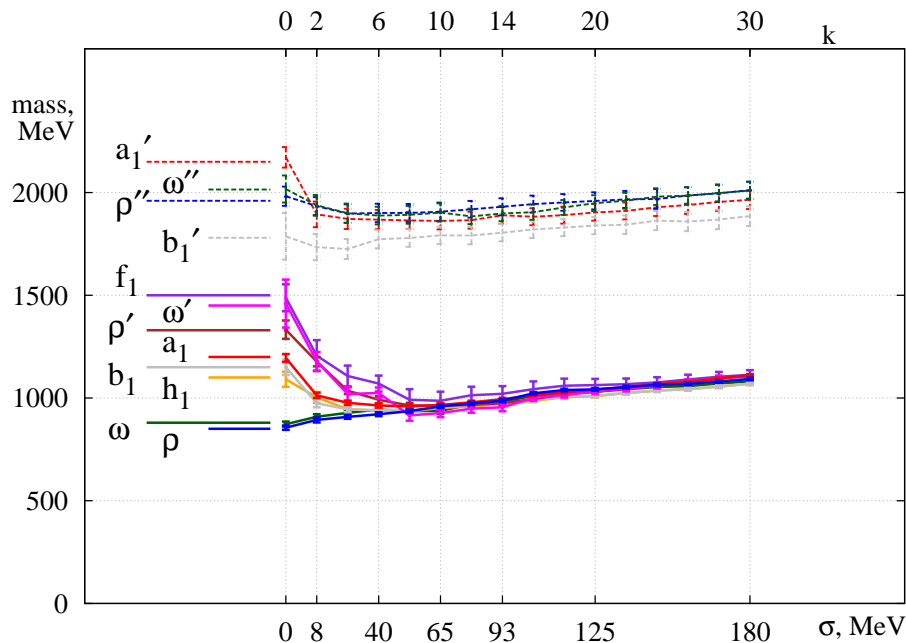


FIG. 13: Mass evolution of $J = 1$ mesons on exclusion of the quasi-zero modes. The value σ denotes the energy gap.

a color-magnetic field in the system and could be interpreted as a manifestation of a dynamical string in QCD_r .

IV. CONCLUSION

We have studied all possible $\bar{q}q$, $J = 0, 1$ mesons in a dynamical lattice simulation with the manifestly chirally invariant overlap Dirac operator and their behavior upon reduction of the lowest-lying eigenmodes of the Dirac operator from the valence quark propagators. In the π, σ, a_0, η channels ($J = 0$) we observe a simultaneous restoration of both chiral and $U(1)_A$ symmetries: All possible point-to-point correlators become identical. The ground states of π, σ, a_0, η mesons do not survive the unbreaking, however. They disappear from the physical spectrum of the bound states, because the corresponding correlation functions decay not exponentially.

In the $J = 1$ channels we find in contrast a very clean exponential decay of the correlators. Consequently, the $J = 1$ states survive the unbreaking of the chiral symmetry. After removal of the quasi-zero modes their masses become manifestly chirally symmetric.

In the present case we also have evidence of a simultaneous restoration of both $SU(2)_L \times SU(2)_R$ and $U(1)_A$ symmetries, like in the $J = 0$ channels. In the $J = 1$ channels we clearly see a degeneracy of all eight possible mesons, which signals a restoration of the higher symmetry, the $SU(4)$. The latter symmetry is not a symmetry of the QCD Lagrangian, but is an emergent symmetry that appears from the QCD dynamics upon removal of the close-to-zero Dirac modes. It operates only in $J \geq 1$

mesons. This symmetry suggests an absence of a color-magnetic field and can be interpreted as a symmetry of a dynamical string in QCD_r .

Appendix A: Correlation functions

In this section we present an outline of the meson two-point correlation function computation with stochastic estimation techniques. Here is a list of quark vectors representing quark sources and solution vectors according to [15, 26],

$$\begin{aligned} \{v_k\} &= \left\{ u_1, u_2, \dots, u_{N_e}, x_1, \dots, x_{N_d} \right\} \\ \{w_k\} &= \left\{ \frac{u_1}{\lambda_1}, \frac{u_2}{\lambda_2}, \dots, \frac{u_{N_e}}{\lambda_{N_e}}, P_l \eta_1, \dots, P_l \eta_{N_d} \right\}, \end{aligned} \quad (\text{A1})$$

where u_k are $N_e = 100$ low-lying modes and η_{N_d} single $Z(2)$ noise vector for each configuration. These are diluted into $N_d = 3 \times 4 \times N_t/2$ vectors η_d ($d = 1, \dots, N_d$), which have nonzero elements only for a single combination of color and Dirac indices and at two consecutive time slices. The vectors x_d represent the solution of the linear equation

$$D_{ov}(m)x_d = P_l \eta_d \quad (\text{A2})$$

with a low-mode projector $P_l = 1 - \sum_{n=1}^{N_e} u_n u_n^\dagger$. Next we use these vectors for the evaluation of two-point functions

in the isovector meson channel,

$$\begin{aligned}
& G_{\Gamma}^{I=1}(t; \mathbf{p} = 0) \\
&= \langle (\bar{q}_1 \Gamma q_2)(t) (\bar{q}_2 \Gamma^\dagger q_1)(0) \rangle \\
&= \sum_{n=1}^{N_e+N_d} \sum_{m=1}^{N_e+N_d} \mathcal{O}^{(m,n)}(t) \mathcal{O}^{(n,m)}(0) \\
&= C(t),
\end{aligned} \tag{A3}$$

and in the isoscalar meson channel,

$$\begin{aligned}
& G_{\Gamma}^{I=0}(t; \mathbf{p} = 0) \\
&= \langle (\bar{q} \Gamma q)(t) (\bar{q} \Gamma q)(0) \rangle \\
&= \sum_{n=1}^{N_e+N_d} \sum_{m=1}^{N_e+N_d} \mathcal{O}^{(m,n)}(t) \mathcal{O}^{(n,m)}(0) \\
&- 2 \sum_{n=1}^{N_e+N_d} \mathcal{O}^{(n,n)}(t) \sum_{m=1}^{N_e+N_d} \mathcal{O}^{(m,m)}(0) \\
&= C(t) + D(t),
\end{aligned} \tag{A4}$$

with

$$\mathcal{O}^{(n,m)}(t) = \sum_{\mathbf{r}} \phi(\mathbf{r}) w_m(\mathbf{x} + \mathbf{r}, t) \Gamma v_n(\mathbf{x}, t) \tag{A5}$$

defined as a smeared meson interpolating field at time t with Γ a product of Dirac matrices and smearing functions ϕ . We used an exponential type of smearing functions and Γ structure combinations $\{\phi_s, \Gamma\}$ listed in Tables II and I for $J = 0, 1$ mesons.

s	$\phi_s(\mathbf{r}) \propto$	s	$\phi_s(\mathbf{r}) \propto$
1	$\delta_{\mathbf{r},0}$	8	$ \mathbf{r} e^{- \mathbf{r} }$
2	const	9	$ \mathbf{r} e^{- \mathbf{r} ^2}$
3	$e^{-0.4 \mathbf{r} }$	10	$ \mathbf{r} ^2 e^{-0.2 \mathbf{r} ^2}$
4	$e^{- \mathbf{r} }$	11	$ \mathbf{r} ^2 e^{-0.4 \mathbf{r} ^2}$
5	$e^{-0.4 \mathbf{r} ^2}$	12	$ \mathbf{r} ^2 e^{-0.7 \mathbf{r} ^2}$
6	$e^{-0.7 \mathbf{r} ^2}$	13	$ \mathbf{r} ^2 e^{- \mathbf{r} ^2}$
7	$e^{- \mathbf{r} ^2}$	14-26	$\phi_s = \phi_{1-13}$

TABLE II: Smearing functions with normalization $\sum_r |\phi_s(\mathbf{r})| = 1$

Appendix B: Fit results

Single exponential effective mass fits and corresponding $\chi^2/\text{d.o.f.}$ are presented in Table III. It is possible to optimize the set of interpolators in order to improve the signal of the extracted states and consequently $\chi^2/\text{d.o.f.}$ ratios at each truncation level k of near-zero modes. For the sake of consistency, we present numerical results for masses of mesons obtained with the fixed set of interpolators in each quantum channel for all values of k .

Acknowledgments

We are deeply grateful to S. Aoki, S. Hashimoto and T. Kaneko for their suggestion to use the JLQCD overlap gauge configurations and quark propagators, for their help and hospitality during our visit to KEK. The calculations were performed on computing clusters of the University of Graz (NAWI Graz). Support from the Austrian Science Fund (FWF) through the grants DK W1203-N16 and P26627-N16 is acknowledged.

[1] M. Denissenya, L. Y. Glozman and C. B. Lang, Phys. Rev. D **89**, 077502 (2014);
[2] H. Neuberger, Phys. Lett. B **417**, 141 (1998).
[3] C. B. Lang and M. Schröck, Phys. Rev. D **84**, 087704 (2011).
[4] L. Y. Glozman, C. B. Lang and M. Schröck, Phys. Rev. D **86**, 014507 (2012).

[5] T. Banks and A. Casher, Nucl. Phys. B **169**, 103 (1980).
[6] We have checked that a nonlocality induced by such a procedure is, however, tiny [7].
[7] M. Schröck, M. Denissenya, L. Y. Glozman and C. B. Lang, PoS LATTICE2013, 116 (2013).
[8] L. Ya. Glozman, arXiv:1407.2798 [hep-ph].
[9] S. Aoki *et al.* [JLQCD Collaboration], Phys. Rev. D **78**,

$k = 0$						$k = 12$					
state	n	am	$\chi^2/\text{d.o.f.}$	t	$\{s\}$	state	n	am	$\chi^2/\text{d.o.f.}$	t	$\{s\}$
ρ	1	0.514 ± 0.006	1.37/6	4 - 11	4,5,7,9,	ρ	1	0.585 ± 0.005	13.49/8	4 - 13	4,5,7,9,
	2	0.801 ± 0.027	11.12/4	3 - 8	13,17,18,		2	0.581 ± 0.006	22.22/7	4 - 12	13,17,18,
	3	1.191 ± 0.028	1.66/4	3 - 8	19,22,24		3	1.153 ± 0.024	1.35/3	3 - 7	19,22,24
ω	1	0.524 ± 0.008	4.87/7	3 - 11	4,5,7,9,	ω	1	0.583 ± 0.006	1.92/5	5 - 11	4,5,7,9,
	2	0.877 ± 0.070	1.14/4	3 - 8	13,17,18,		2	0.570 ± 0.012	0.38/4	5 - 10	13,17,18,
	3	1.213 ± 0.040	0.22/2	3 - 6	19,22,24		3	1.133 ± 0.023	3.83/3	3 - 7	19,22,24
a_1	1	0.718 ± 0.012	0.12/5	3 - 9	4,8,9,12,13	a_1	1	0.589 ± 0.005	21.91/8	4 - 13	4,8,9,12,13
	2	1.305 ± 0.030	2.86/3	3 - 7			2	1.121 ± 0.025	2.11/4	4 - 9	
f_1	1	0.894 ± 0.039	1.00/4	3 - 8	5,7,9,11,12	f_1	1	0.609 ± 0.025	0.13/2	5 - 8	5,7,9,11,12
b_1	1	0.691 ± 0.023	0.67/3	3 - 7	4,5,6,7,8,9	b_1	1	0.579 ± 0.005	4.61/6	3 - 10	4,5,6,7,8,9
	2	1.074 ± 0.068	0.14/3	3 - 7			2	1.076 ± 0.026	0.18/3	3 - 7	
h_1	1	0.656 ± 0.022	0.22/3	3 - 7	4,5,6,7,8,9	h_1	1	0.576 ± 0.005	7.03/9	3 - 13	4,5,6,7,8,9
	2	1.064 ± 0.074	0.17/2	3 - 6			2	1.076 ± 0.026	0.20/3	3 - 7	

TABLE III: Results of fits to the eigenvalues at a truncation levels $k = 0, 12$ for $J = 1$ mesons: the states are obtained from smeared interpolating fields. Each of the quantum states is denoted by $n = 1, 2, \dots$. The mass values are in lattice units; t denotes the fit range and $\{s\}$ labels the set of smearing functions (see Table II of Appendix A) used in the construction of interpolating fields with respect to each quantum channel.

- 014508 (2008).
- [10] S. Aoki *et al.* Prog. Theor. Exp. Phys. **2012**, 01A106 (2012).
- [11] S. Aoki *et al.*, Phys. Rev. D **76**, 054508 (2007).
- [12] R. Brower *et al.*, Phys. Lett. B **560**, 64 (2003).
- [13] G. S. Bali *et al.*, Phys. Rev. D **64**, 054502 (2001).
- [14] J. Noaki *et al.* [JLQCD and TWQCD Collaborations], Phys. Rev. Lett. **101**, 202004 (2008)
- [15] S. Aoki *et al.* [JLQCD and TWQCD Collaborations], Phys. Rev. D **80**, 034508 (2009)
- [16] M. Lüscher and U. Wolff, Nucl. Phys. B **339**, 222 (1990); C. Michael, Nucl. Phys. B **259**, 58 (1985); B. Blossier *et al.*, JHEP 04, 094 (2009).
- [17] T. D. Cohen and X. -D. Ji, Phys. Rev. D **55**, 6870 (1997).
- [18] L. Y. .Glozman, Phys. Rept. **444**, 1 (2007)
- [19] T. Kunihiro *et al.*, Nucl. Phys. Proc. Suppl. **186**, 294 (2009)
- [20] K. Hashimoto and T. Izubuchi, Prog. Theor. Phys. **119**, 599 (2008)
- [21] S. Aoki *et al.*, Phys. Lett. B **665**, 294 (2008)
- [22] L. Y. Glozman, Phys. Lett. B **587**, 69 (2004).
- [23] G. 't Hooft, Phys. Rept. **142**, 357 (1986).
- [24] E. V. Shuryak, Nucl. Phys. B **203**, 93 (1982).
- [25] D. Diakonov and V. Y. Petrov, Nucl. Phys. B **272**, 457 (1986).
- [26] J. Foley *et al.*, Comput. Phys. Commun. **172** (2005) 145.